Cooperative Soccer Play by Real Small-Size Robot

Kazuhito Murakami[1], Shinya Hibino[2], Yukiharu Kodama[2], Tomoyuki Iida[1], Kyosuke Kato[2], and Tadashi Naruse[1]

[1] Aichi Prefectural University, Nagakute-cho, Aichi, 480-1198, Japan
[2] Graduate School of Information Science and Technology
Aichi Prefectural University, Nagakute-cho, Aichi 480-1198, Japan
apurobo@ist.aichi-pu.ac.jp
http://www.aichi-pu.ac.jp/ist/lab/narulab/index.html

Abstract. One of the typical cooperative actions is the pass play in RoboCup small-size league. This paper presents three technical key features to realize robust pass play between robots. The first one is the high resolution image processing to detect the positions and orientations of the robots. The second one is the control algorithm to move and adjust the robots for the pass play. The third one is the mechanism to catch the ball moving at high speed. This paper discusses these methods and shows the effectiveness of the methods by experimental results.

1 Introduction

RoboCup gives full scope to realize a soccer game by robot [1–5]. It is important to realize a robust pass play. There are many key features to realize robust pass play between robots. From the viewpoint of software, it is important to realize the high resolution image processing algorithm to detect the positions and the orientations of the robots. If the image processing system couldn't detect moving objects correctly or it would take too much time, it would be impossible to kick and receive the ball at the promised place. A control algorithm to move and adjust both robots for the pass play is also required because the ball would not be passed at the time promised. From the viewpoint of hardware, it is necessary to design a mechanical device to catch the ball moving at high speed, because the ball collides with the robot at high speed and rebounds off to an unexpected direction.

From these considerations, we realized simple but high-speed image processing system whose processing speed is about 1.4 msec to detect and track the robots and a ball by reducing the searching range, and also implemented an algorithm to control both robots, the passing robot and the receiving robot, for the robust pass play. We improved the dribbling mechanism to catch the ball moving at high speed by intentionally adding some loose to the joint part of the dribbling device.

In the following, the image processing system and cooperative algorithm to realize a pass play are shown in sections 2 and 3, respectively. The mechanical devices to catch the ball and its modeling are shown in section 4.

D. Polani et al. (Eds.): RoboCup 2003, LNAI 3020, pp. 410–421, 2004.

2 Image Processing System

2.1 Objects to Be Detected

It is allowed to attach other submarkers to detect the identity number (ID) of each robot and/or the orientation of the robot. The number, size and layout of submarkers are unrestricted but approved colors are limited so as not to affect the robotic image processing systems used by opposing teams. Figure 1 shows submarkers of our team. A rectangle submarker (105mm× 16.5mm) has been used to determine the orientation of the robot, and small circle submarkers (1∼ 4 pieces, 8.5mm diameter) have been used to determine ID of each robot. Our image processing system aimed to detect these markers.

2.2 Image Processing System

CPU in the host computer is a Pentium Xeon 2GHz and the OS is Windows 2000. We employ a progressive scanning camera (DXC-9000, SONY) to avoid the problem of the difference between the odd frame and the even frame caused by the high-speed movement of the robot.

Global vision camera is set at 3.0m over the game field. Since the length along to the side-line including the goal area becomes about 3.2m, at least 56 degree view angle is needed. In our system, wide lens attachment (Fujinon, WCV-65, × 0.75) covers this range. The size of the global vision image grabbed by the frame grabber (Matrox, GEN/X/00/STD) is 640(W)×480(H), and the resolution is 5 mm/pixel.

Fig. 1. Top surface of robot

2.3 Image Processing Algorithm

Image processing system detects the location of each robot by using team color markers, and determines the orientation and the ID number (code) of each robot by using submarkers attached on the top of the robot. Figure 2 shows the flowchart of image processing. The outline of processing is shown below and literatures [6–9] give detailed description.

Step-1 (Input Image) Get an RGB image from frame grabber which is captured through the progressive camera. Figure 3 shows an example of input image. Figure 3(b) is the enlarged images around the robots.

Step-2 (Calculation of Search Range) Calculate the search range based on the reliability of respective objects. Since the reliability is an important parameter which characterizes the performance of image processing, the details of the calculation are explained later in this section. White rectangles around robots in Fig.4 are the search ranges. Only in these ranges, RGB color format image is converted to YUV color format image. This greatly reduces computation time.

Step-3 (Segmentation of Colored Region) In the same ranges as restricted in Step-2, the simultaneous pattern matching is executed for 9 colors (max. 32colors) in YUV color format image by using the CMU's color segmentation algorithm[10]. Since the real game is not played under the uniform light conditions, the intensity and color spectrum are not uniform over the game field. Therefore, we assign several colors as a candidate for the object. We assign 2 colors for the ball, 2 colors for each team color and 3 colors for the areas that we would like to remove from processing. This method realizes the robust color extraction under the non-uniform lighting conditions.

Step-4 (Labeling) Apply the first propagation in the labeling algorithm, which we have developed last year[9], to label the object region. Figure 5 shows the result. In this algorithm, the processing for interlaced image is not applied, since we use non-interlaced image.

Step-5 (Selection of Objects) Detect team marker region and expand the region. Then, detect ID markers and rectangle submarker in the expanded region. ID markers area and rectangle submarker area are distinguished by the size of area. Figure 6 shows the result.

Step-6 (Calculation of IDs and Directions) Calculate the ID and the rough orientation of the robot by the numbers and the positions of circle submarkers, respectively. The precision for the angle is about 8 degrees.

Step-7 (Calculation of Modified Directions) Calculate the precise orientation of the robot by detecting the long-side edges of rectangle submarker and applying the least mean square method to the detected edges. The precision goes up to less than 1 degree.

Step-8 (Record of Positions and Directions) Record the current positions and directions.

Step-9 (Output of Object IDs, Positions and Directions) Convert the objects positions from the camera coordinates to the world coordinates.

We utilize the reliability factor to decide the search range in Step-2 and Step-3. Reliability indicates how much the result of image processing is correct. Wide range should be searched if the reliability is low. On the contrary, it is enough to search in the restricted range if the reliability is high.

We defined 4 levels of reliability, i.e. non-, low-, intermediate- and high-reliability level. The reliability level is updated every frame cycle (i.e. 60 times per second). Basically, it goes up 1 level if the object detection ends in success, otherwise goes down 1 level.

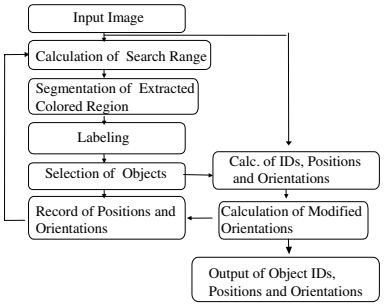

Fig. 2. Flowchart of image processing

The decreasing of the reliability level makes the search range wider and causes the increasing of computation time. However, information management system prevents the reliability level from excessive go-down. Such cases happen when the ball is occluded, since the ball detection ends in failure. The information management system keeps the reliability level at 2 (intermediate).

The search range is restricted when the reliability level is in 1–3, i.e. the range of 20 × 20 pixels, 30 × 30 pixels and 60 × 60 pixels is searched when the reliability level is 3, 2 and 1, respectively. 20 × 20 pixels range is about 10 cm × 10 cm in the real field. This search range works for the tracking of a moving object up to 3m/sec.

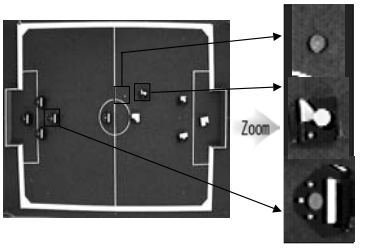

(a) global vision image (b) enlarged image

Fig. 3. An example of grabbed image from a global vision camera

3 Cooperative Control Algorithm

There are many types of cooperative play in our system, for example, pass-play, defense-play, assist-play and so on. In this paper, we discuss the pass play algorithm. Algorithms for passing robot and receiving robot are given below.

First, we define variables and flags. Let the line connecting the center of passing robot and the receiving robot be $Line_A$, and let the line on the heading direction of passing robot be $Line_B$. Let the angle between $Line_A$ and $Line_B$

Fig. 4. Restricted region to be searched (whitened area) and enlarged images

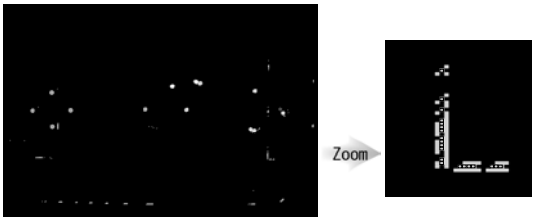

Straight lines of width 1 pixel will be recognized as separated objects. They are easily removed by area thresholding.

Fig. 5. An example of line noises to be deleted by the proposed labeling algorithm

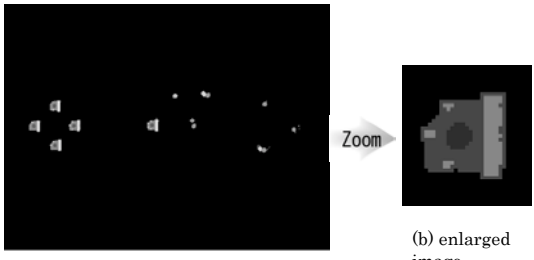

(a) the result of marker extraction

(b) enlarged image

Fig. 6. The result of marker extraction

be θ . Let the direction flag and stabilization flag be Dir and $PassCounter$, respectively.

[Initializing]

Step 1 Decide the rotation speed v_r based on the velocity profile shown in figure 7. v_r depends on θ. Start rotation.

Step 2 Start dribbling device.

Step 3 If there is an obstacle on $Line_A$, then compute which side of $Line_A$ the center of that obstacle is located. If it located on left-hand side of the passing robot, then set Dir to 1, otherwise -1. If there is no obstacle on $Line_A$, then set Dir to 0.

[Pass Algorithm]

Step 1 Do the Initializing.
Step 2 If Dir is not 0, then set $PassCounter$ to 0 and go to Step 5.
Step 3 Go along $Line_B$ at a speed of v_{ps}.
Step 4 If $|\theta|$ is less than θ_{ps} and the distance between the ball and the passing robot is less than d_{min}, then increase $PassCounter$ by 1. If $PassCounter$ is greater than n_ps and $|\theta|$ is less than θ_{min}, then start the kicking device. Reset $PassCounter$.
Step 5 Wait for the next frame cycle. Go to step 1.

In the above, $v_{ps}, \theta_{ps}, d_{min}, n_{ps}, \theta_{min}$ are constants and are determined by the experiments.

[Receive Algorithm]

Step 1 Do the Initializing.
Step 2 If Dir is not 0, then go in the direction of $Dir \times \theta_{rec}$ from $Line_B$ at a speed of $\min(v_{rec}, c_{rec} \times distance\_between\_ball\_and\_Line_A)$.
Step 3 Wait for the next frame cycle. Go to Step 1.

In the above, $v_{rec}, \theta_{rec}, c_{rec}$ are constants and are determined by the experiments.

4 Catching Mechanism and Its Analysis

4.1 Robot Mechanism

The robot must be constructed in order to execute the commands, such as a move, a shoot and a dribble. Figure 8 shows our robot. Our robot has 3 omni-wheels and can move any direction. As shown in Fig.8 (a), 3 DC motors with encoders are used (FAULHAVER). The gear ratio is 9.7:1. The kicking device that is driven by a solenoid (SINDENGEN) is mounted (Fig.8 (a) below). It can kick the ball at the maximum speed of about 3m/sec. Dribbling device utilizes the rotating roller to give backspin to the ball. Uncovered robot in Fig.8 (b) shows dribbling roller.

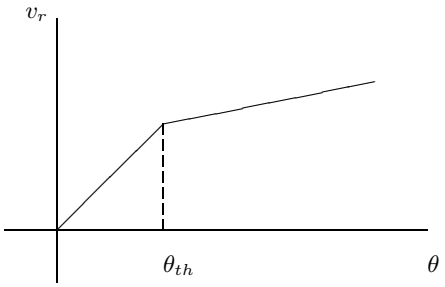

Fig. 7. Velocity profile

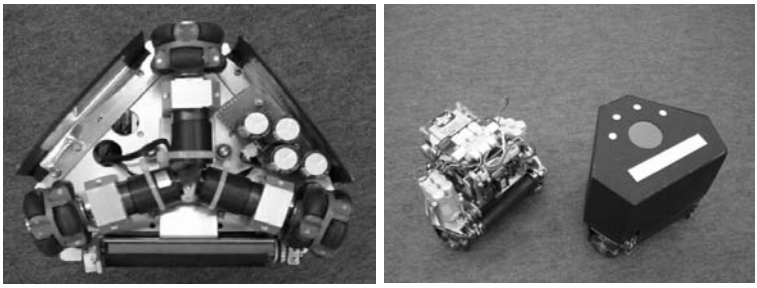

(a) omni-directional drive.

(b) appearance of our robot.

Fig. 8. Our robot system

There are two important technical issues to realize a pass play. One is the correct recognition of the position and the orientation of each robot and the ball. The other is the mechanical improvement to catch the ball. For the former, our precise and high-speed image processing system solved the problem as described in section 2, and for the latter subject, our system solved the problem by adding shock absorption mechanism to the dribbling device. It may be natural to use a spring like the Cornell University's BigRed, but our team realizes it by another method.

The dribbling device is attached in front of the robot as shown in Fig.8 (b). The roller made of rubber rotates and gives backspin to a given ball and holds the ball. However, because the roller is hard enough not to bite into the ball which is also hard, the ball will bounce off of it if the dribbling device receives the fast ball. To solve this problem, we made the joint of the roller looser than normal and making it possible for it to move upward slightly. This simple looser joint enables the impact of the ball to be sufficiently absorbed. Still, it remains necessary to adjust the degree of looseness depending on the quality on the surface of the carpet on the robotic soccer field.

4.2 Modeling of Catching Device

There are so many factors to model real shock absorption mechanism. Since our system realizes it by adding adequate space to the joint of the dribbling roller, we analyzed it by three simplified models, (a) at the impact, (b) transition to the stable state, and (c) in the stable state.

(a) Impact Model

Let the angle between the horizontal line and the line crossing to the centers of the roller and the ball be θ, and let m_R and m_B, ν_R and ν_B be mass and velocity of the roller and the ball, respectively, in the world $X-Y$ coordinates as shown in Fig.9. Let the components of ν_R and ν_B be $(\nu_{R,x}, \nu_{R,y})$ and $(\nu_{B,x}, \nu_{B,y})$ in the local $x-y$ coordinates parallel to the tangent line and the normal line at the collision point as shown in Fig.9.

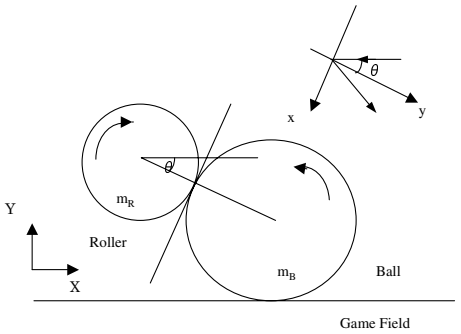

Fig. 9. Physical situation at a the impact

First, by modeling the collision without rotation of the roller and the ball by the law of conservation of moment, following equations for the y-coordinate,

$$\nu_{B,y}^{'} - \nu_{R,y}^{'} = -e_y(\nu_{B,y} - \nu_{R,y}) \tag{1}$$

$$m_B\nu_{B,y} + m_R\nu_{R,y} = m_B\nu_{B,y}^{'} + m_R\nu_{R,y}^{'} \tag{2}$$

are obtained, here dash denotes the velocity after collision and e_y is the coefficient of rebound for y-coordinate. As the same way for x- coordinate,

$$\nu_{B,x}^{'} - \nu_{R,x}^{'} = e_x(\nu_{B,x} - \nu_{R,x}) \tag{3}$$

$$m_B\nu_{B,x} + m_R\nu_{R,x} = m_B\nu_{B,x}^{'} + m_R\nu_{R,x}^{'} \tag{4}$$

are obtained, and the collision of ball and roller is modeled when they are assumed as a particle.

Since the roller and the ball are rotating, it is necessary to introduce some equations concerning to the angular momentum. Let the moment of inertia and angular velocity be I and ω, respectively. From the law of conservation of angular momentum,

$$I_B\omega_B + I_R\omega_R = I_B\omega_B^{'} + I_R\omega_R^{'} \tag{5}$$

and following equations,

$$r_B\omega_B = \nu_{B,x}\ ,\ r_R\omega_R = \nu_{R,x}\ ,\ r_B\omega_B^{'} = \nu_{B,x}^{'}\ ,\ r_R\omega_R^{'} = \nu_{R,x}^{'} \tag{6}$$

are realized at the collision point, here, r_B, r_R are the radius of the ball and roller, respectively. Since our system utilizes rubber of cylinder, the moments of inertia I_R and I_B are easily calculated as $I_R = \frac{1}{2}r_R^2 m_R$ and $I_B = \frac{2}{5}r_B^2 m_B$, respectively. The solutions of $\nu_{R,x}^{'}$, $\nu_{R,y}^{'}$, $\nu_{B,x}^{'}$, $\nu_{B,y}^{'}$ at the impact are calculated by solving equations (1) $\sim$ (6).

(b) Transition Model

The center of gravity of the ball repeats the reflection after the impact as shown in Fig.10. It is sufficient to consider the movement of the center if the angle θ

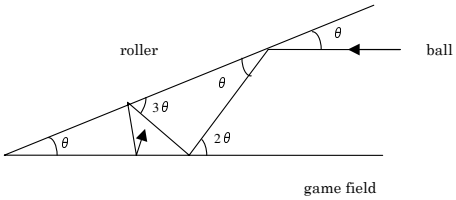

Fig. 10. Reflections of ball in the transition

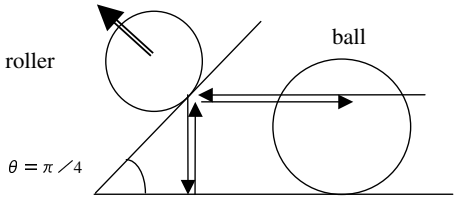

Fig. 11. An example of shock absorption at $\theta = \pi/4$

varies within the range of a few degree during the transition. Precise analysis and modeling are one of our future works, but it is possible to realize simple model as follows if the relation $e_x \equiv e_y$ is satisfied in the $x-y$ local coordinates.

Reflection angle increases reflection by reflection as shown in Fig.10, namely $\theta, 2\theta, 3\theta, ..., n\theta, ...$. After n times reflections, it exceeds $\pi/2$ and the ball returns back to the inverse direction. Figure 11 shows the case of $\theta = \pi/4$. In this case, the ball rebounds in a short time and if the roller moves to the direction illustrated with arrow in order to absorb the shock, these angular relations are satisfied during transition.

(c) Stable Model

Let the reactions be N_B, N_R and let the coefficients of kinetic friction be μ_1, μ_2 as shown in Fig.12. The equations of motion for the ball are as follows.

$$\text{For X} - \text{direction}: \quad -\mu_1 N_B + N_R \cos\theta - \mu_2 N_B \sin\theta = 0 \tag{7}$$

$$\text{For Y} - \text{direction}: \quad N_B - m_B g - N_R \sin\theta - \mu_2 N_R \cos\theta = 0 \tag{8}$$

By solving equations (7) and (8), the solutions for N_B, N_R are obtained as follows.

$$N_R = \frac{\mu_1 m_B g}{-(\mu_1+\mu_2)\sin\theta + (1-\mu_1\mu_2)\cos\theta} \tag{9}$$

$$N_B = \frac{(\cos\theta - \mu_2 \sin\theta) m_B g}{-(\mu_1+\mu_2)\sin\theta + (1-\mu_1\mu_2)\cos\theta} \tag{10}$$

So the force by backspin of the ball is derived as

$$\begin{aligned} f = \mu_1 N_B &= \frac{\mu_1(\cos\theta - \mu_2\sin\theta) m_B g}{-(\mu_1+\mu_2)\sin\theta + (1-\mu_1\mu_2)\cos\theta} \\ &= \frac{\mu_1(1-\mu_2\tan\theta) m_B g}{1-\mu_1\mu_2 - (\mu_1+\mu_2)\tan\theta} \end{aligned} \tag{11}$$

From equation (11), following equations are obtained.

$$\frac{\partial f}{\partial \theta} = \frac{\mu_1^2(1+\mu_2^2)m_B g}{\{1-\mu_1\mu_2-(\mu_1+\mu_2)\tan\theta\}^2\cos^2\theta} \tag{12}$$

$$\frac{\partial f}{\partial \mu_1} = \frac{(1-\mu_2\tan\theta)^2 m_B g}{\{1-\mu_1\mu_2-(\mu_1+\mu_2)\tan\theta\}^2} \tag{13}$$

$$\frac{\partial f}{\partial \mu_2} = \frac{\mu_1^2(1+\tan^2\theta)m_B g}{\{1-\mu_1\mu_2-(\mu_1+\mu_2)\tan\theta\}^2} \tag{14}$$

It is easily known that larger force f could be obtained according to the increase of θ because $\frac{\partial f}{\partial \theta} > 0$ and $f|_{\theta=0} > 0$. It is important that f has a critical point at $\theta = \arctan\frac{1}{\mu_2}$. At this point, f becomes 0.

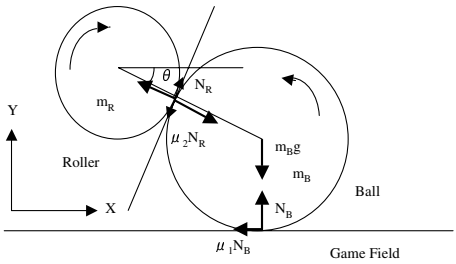

Fig. 12. Stable model by dribbling device

5 Considerations

From the viewpoint of mechanical performance, we confirmed the effectiveness to use the dribbling and kicking devices. Dribbling device worked well except for the case that the coefficient of kinetic friction of the field's carpet is high and the robot lost a ball around the wall of the game field.

For the performance of image processing system, it was experimentally confirmed that the angle accuracy is sufficient to realize cooperative play. Experimental results are shown in Table 1 under the condition that two incandescent lights are added to the fluorescent lights for making the environment near the actual game hall. As a result, the luminosity value on the game field was set to 450-800 lux. In the ID detection experiment, five robots have been placed at the free kick markers and at the center on the field, and each robot's ID was recognized 10,000 times under the condition that the robots do not move. If the distance between the recognized position of robot and its planned position is less than 10cm, the recognition is succeeded, otherwise failed.

The accuracy of angle detection is experimented on nine points on the field and the orientation of the robot was set to 0, 45, 90 and 135 degrees at each setting point. It was measured 1,000 times at each point, and the maximum

angle error was calculated from the real position. There is no weak point (place) on the field to detect ID's and submarkers.

The recognition rates for the objects, ball, team color marker, submarkers, are evaluated during a real game. Although the intensity on the field is determined as 700–1000 lux by the regulation, it varies by the lighting condition. From some practical games, it is confirmed that our image processing system could extract all objects under the condition that the intensity is about 200 lux.

In our image processing system, the whole image was searched only when (1) just after the game started, (2) ball has been occluded completely for some period, and (3) shoot speed exceeds 5m/sec. Even though it takes long time for the whole image search, it is confirmed that it works in 20msec/frame. So that, our system could defend a fast ball even if it was shot from the region occluded by a robot.

Table 1. Experimental results of image processing performance

Experimental item	Planned	Result
ID recognition ratio in a static mode [%]	100.00	99.68
ID recognition ratio in a dynamic mode [%]	100.00	99.61
Maximum deviation for the position [cm]	0.50	0.097
Maximum deviation for the angle [deg]	1.00	0.78
Processing time [msec]	16.7	1.33

6 Conclusions

This paper discussed the algorithms, the robot mechanism and image processing method to realize cooperative play in RoboCup small-size league. Key features in our system are simple pass algorithms, implementation of dribbling and kicking devices, and high speed and robust image processing method. In particular, the visual feedback system of every 1/60 seconds realized high speed tracking to the ball moving at 3.0m/sec. From the viewpoint of image processing, if the light includes wide spectrum like natural light, more robust method will be required, because color blur appears around the boundary of the object to be detected by optical color aberration. The light with too wide dynamic range like a spot light bothers our image processing system, so it is also required to be more robust for the change of the intensity, exceeding the value specified in the regulation. From the view point of mechanism, further analysis and modeling of catching and shock absorption are expected. These are future works.

Acknowledgement

This paper was partially supported by The Hibi Research Grant, AI Research Promotion Foundation and the RoboCup Japanese Committee grant.

References

1. http://www.robocup2002.org/
2. M.Veloso, E.Pagello, and H.Kitano (Eds.), "RoboCup-99: Robot Soccer WorldCup III", Springer (June 2000)
3. P.Stone, T.Balch and G.Kraetzschmar (Eds.), "RoboCup 2000:Robot Soccer WorldCup IV", Springer (March 2000)
4. A.Brik, S.Coradeschi, and S.Tadokoro (Eds.), "RoboCup 2001:Robot Soccer WorldCup V", Springer (March 2002)
5. G.A.Kaminka, P.U.Lima and R.Rojas (Eds.), "RoboCup 2002:Robot Soccer WorldCup VI", The 2002 International RoboCup Symposium PreProceedings, Fukuoka, (June 2002)
6. Y.Kodama and K.Murakami, "Small-Size Robot Extraction Method by High-speed Image Processing for RoboCup", Proc. of VIEW2002, Yokohama, (Dec.2002) (In Japanese)
7. S.Hibino, Y.Kodama, T.Iida, K.Kato, S.Kondo, K.Murakami, and T.Naruse, "System configuration of RoboDragons team in RoboCup small- size league", Proc. of SI2002, Kobe, (Dec.2002) (In Japanese)
8. Y.Kodama, S.Hibino, K.Murakami, and T.Naruse, "Small Robot Detection by Using Image Processing and its Application to Action Planning and Action Analysis", Proc.of MIRU2002, Vol.1, pp.223-228, Nagoya, (July 2002) (In Japanese)
9. S.Hibino, Y.Kodama, Y.Nagasaka, T.Takahashi, K.Murakami, and T.Naruse, "Fast image processing and flexible path generation system for RoboCup small size league", The 2002 International RoboCup Symposium Pre-Proceedings, pp.45-57, Fukuoka, (June 2002)
10. Bruce, J., Balch, T. and Veloso, M.: "Fast and Inexpensive Color Image Segmentation for Interactive Robots", Proc. of IROS '00, pp. 2061-2066 (2000)